



Toward the constitutive modeling of epoxy matrix: Temperature-accelerated quasi-static molecular simulations consistent with the experimental test

Hyungbum Park^a, Joonmyung Choi^{a,b}, Byungjo Kim^a, Seunghwa Yang^c, Hyunseong Shin^{a,b}, Maenghyo Cho^{a,b,*}

^a Division of Multiscale Mechanical Design, School of Mechanical and Aerospace Engineering, Seoul National University, Republic of Korea

^b Institute of Advanced Machines and Design, Seoul National University, San 56-1, Shillim-Dong, Kwanak-Ku, Seoul 151-744, Republic of Korea

^c School of Energy Systems Engineering, Chung-Ang University, Seoul 156-756, Republic of Korea

ARTICLE INFO

Keywords:

Quasi-static
Yield
Amorphous polymer

ABSTRACT

We propose an efficient simulation-based methodology to characterize the quasi-static (experimental low strain rate) yield stress of an amorphous thermoset polymer, which has generally been considered a limitation of molecular dynamics (MD) simulations owing to the extremely short time steps involved. In an effort to overcome this limitation, the temperature-accelerated method – in which temperature is treated as being equivalent to time in deformation kinetics – is employed to explore the experimental strain rate conditions. The mechanical tensile behavior of a highly crosslinked polymer is then investigated with MD simulations by considering different strain rates and temperatures below the glass transition temperature. The derived yield stress represents the time- and temperature-dependent characteristics, showing that the yield stress decreases with increasing temperature and decreasing strain rate. Changeable vertical and horizontal shift factors are introduced for the first time to reflect nonlinear characteristics of the yield stress across a broad range of strain rates and to quantify the correlation between increasing temperatures and decreasing strain rates. With the proposed method, the Eyring plot, which describes the rate effect on yield from quasi-static to high-rate conditions, is predicted from MD simulations, and agrees well with macroscopic experimental results. From the constructed Eyring plot, the experimentally validated quasi-static stress-strain response is also estimated by using linear elastic model and Ludwick's hardening model. The proposed method provides new avenues for the design of glassy polymers using only fully atomistic MD simulations, thus overcoming the existing temporal scale limitations.

1. Introduction

Owing to the unique crosslinked molecular network structures between polymer chains, amorphous thermoset polymers have been widely used in various applications that require high performance, light weight, and structural robustness. Since the macroscopic properties – such as elastic modulus, yield strength, toughness, and the glass transition temperature – can be readily tailored by adjusting microscopic parameters (including the molecular structure of resin and crosslinker, molecular weight, conversion ratio, etc.), thermoset polymers currently attract significant interest in industries that rely on advanced materials and high-performance polymers [1–5].

Among various thermoset polymers, epoxy is the most widely used one – not only as an independent functional material, but also as a host matrix for composites and nanocomposites [6–8]. Because of the recent advances in computational methods, which can be applied for modeling condensed matter, theoretical simulations of epoxy polymers have been

recently performed by using various molecular mechanics [9,10], molecular dynamics (MD) [11–14], Monte Carlo [15,16], and density functional theory [17,18] methods.

It is generally agreed that it is difficult to investigate the effects of individual design variables related to nanoscale physics and the segmental motion of epoxy solely by using experiments that demand a tremendous amount of trials and errors. Moreover, limitations in the precise control of the conversion ratio, visualization of the network structure, measurement of free volume related to the aging and degradation, and inevitable measurement noise make it difficult to fully understand the designed epoxy. Therefore, the above-mentioned computer simulation techniques have also aimed at designing high-performance epoxies. In particular, MD simulations are considered to be the most effective and efficient way of probing the internal molecular structure and predicting the physical properties of thermoset polymers. Several groups have proposed specific modeling procedures to describe the real structural characteristics of bulk thermosetting polymers and

* Corresponding author. Division of Multiscale Mechanical Design, School of Mechanical and Aerospace Engineering, Seoul National University, Republic of Korea.
E-mail address: mhcho@snu.ac.kr (M. Cho).

have estimated their thermo-mechanical properties [11–14]. For instance, Kim et al. observed the effect of the crosslink density on thermo-mechanical properties such as the density, elastic modulus, and coefficient of thermal expansion with respect to different crosslinking methods from the point of view of modeling [13]. Li et al. observed the evolution of the molecular structures of two thermosetting epoxy systems with different degrees of cure; they then derived various thermo-mechanical properties, including the yield and glass transition temperature [14].

Moreover, MD simulation studies on epoxy have been a part of the constitutive modeling of composites, especially for the modeling of nanocomposites, which requires the elucidation of important nanoscale characteristics related to their interface or interphase features [19–26]. In this regard, various thermo-mechanical properties of epoxy have been predicted and used to establish constitutive models that are essential in composite micromechanics theories.

While MD simulations play an important role in identifying nano-phenomena under diverse physical situations for amorphous polymer-based materials, the extreme thermo-mechanical loading demands thorough consideration of polymer yielding in order to guarantee and further extend their engineering applications. Prior to the computational approaches in polymer design, the molecular theoretical description for the yield of amorphous polymers was developed from several points of view. Based on the Arrhenius formulation for reaction rates, Eyring first described the yielding of polymer chains as a process of viscous plastic flow induced by the transition that is thermally activated between different equilibrium states on the potential energy surface [27]. Eyring's theory contributed to the deformation kinetics of amorphous polymers, and acted as the foundation of transition state theory. Robertson [28] asserted that the conformational change in the molecules is the origin of polymer chain flow, and that the fraction of high-energy *cis* conformation is maximized through the effect of shear stress on the polymer chains, culminating in the initiation of yield. In addition to the mechanistic explanations of Eyring and Robertson, alternative models for the yielding of polymers – which rely on the concepts of dislocations and disclinations from the deformation mechanisms of conventional crystalline materials – were suggested by Bowden and Raha [29], and Argon [30,31]. More specifically, Bowden considered the origin of yield as small shear strain region, which is analogous to a dislocation loop. On the other hand, Argon noted that the creation of kinks in the polymer chain gives rise to the rearrangement of internal structures, thereby changing the potential energy of the polymer. Recently, studies on the yielding mechanisms have been extended with the aid of computational approaches that enable the direct observation of the plastic behavior of amorphous polymers at the atomic scale [4,32,33].

Although MD simulations have been effectively used in establishing the fundamental background of the elasto-plastic deformation behavior of amorphous polymers, the temporal scale problem arising from extremely short time step, which stems from the computational limitations in the time integration of the equations of motions to obtain quasi-static mechanical response of polymers, remains a challenging issue. It has been generally agreed that in both experimental [34–41] and simulation studies [4,42–44], the yielding of an amorphous polymer is a rate-dependent phenomenon because of its viscoelastic nature; thus yield stress increases with the increasing strain rate. Therefore, owing to the huge time scale gap between the experimental and computational contexts, it is inevitable that notable differences will be observed in the evolution of deformation, which results in quantitative discrepancies of the stress-strain response. The most commonly used strategy that can be used to resolve this problem is coarse-graining [44] by reducing the number of the degrees of freedoms in full-atomic MD simulations. Nonetheless, coarse-graining still requires sophisticated parameter fitting without losing geometric information concerning all atoms. Therefore, an alternative acceleration method to account for the effect of the strain rate on the yielding of polymers is required in order to

reduce the gap between mechanical response predicted by simulation and realistic macroscopic behavior over multiple temporal scales.

In this study, inspired by the abovementioned requirements, we propose an efficient temperature-accelerated method for MD simulations to predict the elasto-plastic behavior of an epoxy polymer across a wide range of strain rates, including quasi-static (experimental low strain rate) conditions. By establishing a correlation between the temperature and strain rate on the basis of transition state theory, the time (strain rate)-temperature superposition method (with incorporated shift factors) is developed to predict the yield strength of epoxy at various strain rates without losing geometric information at the atomic scale. From the uniaxial tensile simulations, the stress-strain responses of crosslinked epoxy are derived at various temperatures and strain rates. In addition, changeable shift factors (corresponding to variations of temperature and strain rate) are introduced to take into account inherent nonlinear characteristics of the epoxy yielding. Together with constructed Eyring plot from suggested accelerated method, quasi-static stress-strain response is also predicted and validated with experimental results.

2. Models and methods

2.1. Theoretical model

To account for the quasi-static mechanical behavior, which is not available in classical MD simulations, we also utilize the concept of temperature-accelerated dynamics (TAD). According to Eyring's model and extended models [45,46], it is revealed that negative temperature dependency and positive strain rate dependency are directly associated with the yielding of glassy polymers. Therefore, if a proper quantitative characterization is enabled between the strain rate and yield strength, and between the temperature and yield strength, the limitation in enlarging the time scale required to consider the slow strain rate within the available Eyring plot can be overcome. The TAD model enables the acceleration of the transition from one state to other states by incorporating thermal activation energy to promote the transition. In combination with transition state theory and the concept of TAD, the inherent time scale limitation of MD simulations can be overcome by elevating the simulation temperature.

As a representative model for describing the polymer yield on the basis of transition state theory, the Ree-Eyring model [45] (modified from the Eyring equation for yield stress) was suggested as follows:

$$\frac{\sigma_y}{T} = A_\alpha \left(\ln(2C_\alpha \dot{\epsilon}) + \frac{Q_\alpha}{kT} \right) + A_\beta \cdot \sinh^{-1} \left(C_\beta \dot{\epsilon} \exp \left(\frac{Q_\beta}{kT} \right) \right), \quad (1)$$

where σ_y , T , k , and $\dot{\epsilon}$ are the yield stress, temperature, Boltzmann constant, and strain rate, respectively. Q_i ($i = \alpha, \beta$) is the activation energy corresponding to the two rate processes of α and β , and A_i and C_i are activation constants. In this model, the strain rate and temperature dependencies on the yield stress are described quantitatively by the activation parameters. While Eyring's initial equation (which fails to describe the yield behavior across a broad range of temperatures and strain rates) considered one rate process to predict the yield stress, the Ree-Eyring model can accurately predict the nonlinear relationship between $\frac{\sigma_y}{T}$ and $\log \dot{\epsilon}$. To accomplish this within a broad temperature range, the yield stress is defined in Eq. (1) by introducing the additional nonlinear strain rate-dependent process β via an arc-hyperbolic sine function.

In addition, Bauwens-Crowet et al. [40] introduced shifting factors (S_x and S_y) on the Ree-Eyring model following the linearized Arrhenius equation:

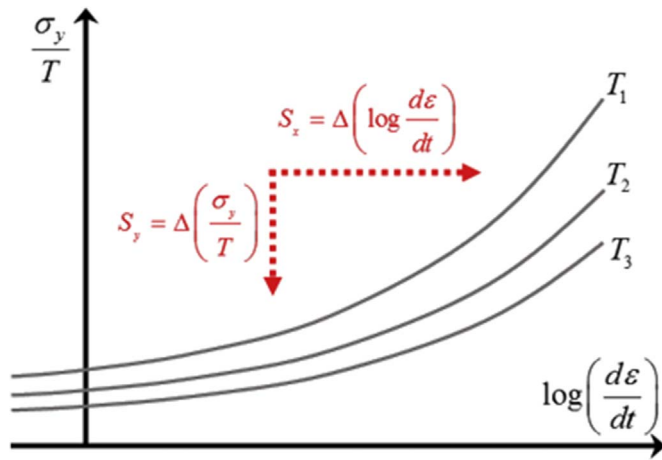


Fig. 1. Eyring plots constructed at three different temperatures ($T_1 < T_2 < T_3$) and effects of the shift factors (reproduced from Ref. [37]).

$$\begin{cases} \Delta \log \dot{\epsilon} = S_x \left(\frac{1}{T} - \frac{1}{T_{ref}} \right) \\ \Delta \frac{\sigma_y}{T} = S_y \left(\frac{1}{T} - \frac{1}{T_{ref}} \right) \end{cases} \quad (2)$$

where T_{ref} is the reference temperature used to determine the shifting factor, which in turn is used to determine the variation in strain rate and yield strength at temperature T . To utilize Eq. (2) in predicting the strain rate–yield strength relationship of glassy polymers at various temperatures, one master curve is obtained from experimental tension or compression tests at the reference temperature. By measuring the activation energy from the constructed curve, the shifting factors can be readily determined [40,41]. Then, according to the values of the two shifting factors and their ratio, the curve of the reduced yield stress $\frac{\sigma_y}{T}$ versus $\log \dot{\epsilon}$ is extrapolated from the master curve, as shown in Fig. 1 [37]. In our simulation study, instead of measuring the activation energy, we propose a novel approach, which uses the slope of a reduced yield profile to determine the shift factor.

2.2. Molecular modeling of amorphous thermoset polymers

In order to prepare the molecular model of the thermoset polymer used in this study, Materials Studio[®] 5.5 commercial software package and parallel molecular dynamics code, Large Atomic/Molecular Massively Parallel Simulation (LAMMPS) were used in consecutive order. In all modeling processes and simulations, a polymer consistent force field (PCFF) was employed to describe the inter- and intra-molecular potentials. An amorphous unit cell consisting of triglycidyl-amino-phenol (TGAP) as an epoxy resin and diamino-diphenylsulfone (DDS) as a curing agent was prepared using the Amorphous Cell module with a target density of 1.2 g/cm³; periodic boundary conditions were imposed on the prepared unit cell in all three directions. The size of the unit cell was 44.68 Å, the epoxy model consisted of a total of 8505 atoms. The details of the molecular structures and the constructed unit cell are presented in Fig. 2. Prior to the crosslinking procedure, epoxy resin and curing agent were dispersed amorphously in a unit cell with a ratio of 4:3 in order to match the stoichiometric conditions determined by having an equal number of reactive sites in epoxy resin and curing agent. After the amorphous cell construction, the model was minimized through the conjugate gradient method and equilibrated through an NVT isothermal ensemble simulation at 500 K for 1 ns to guarantee sufficient chain relaxation and dispersion before the crosslinking procedure.

There have been continuous efforts to obtain a properly crosslinked and network of molecular dynamics model with more advanced and robust algorithms [47–49]. For example, Demir et al. [48] developed

reliable crosslinking procedure of epoxy for calculation of partial atomic charges and equilibration of liquid precursor. Tam et al. [49] also proposed an effective dynamic crosslinking algorithm to construct accurate crosslinking network of photoresist material.

Herein, the crosslinking procedure between the reactive atoms of the resin and the hardener was conducted using a dynamic crosslinking method, which was originally introduced and applied by Heine et al. [47] and Varshney et al. [11] (see Fig. 3). The basic concept of this method consists of monitoring the distance between all reactive pairs of an epoxy resin and a curing agent and forming covalent bonds when a certain distance criterion is satisfied. At every step, the geometric optimization is performed using a conjugate gradient method. Until the predefined crosslink conversion ratio is reached, the cutoff distance is gradually increased to include more candidate atoms in the distance criterion, after which the conversion ratio is computed iteratively. During crosslinking, an energy relaxation procedure is performed via an NVT ensemble simulation to reduce residual stress and ensure local structural rearrangement in the epoxy system after the iterative formation of new crosslinks.

After the crosslinking simulation is complete, the unit cell is equilibrated for a prolonged time through the NVT and NPT ensemble dynamics routines of LAMMPS. In order to achieve a more locally relaxed structure via supplying high thermal energy, an NVT ensemble simulation is performed for 1 ns at 500 K prior to the relaxation at the target temperatures. Afterwards, the same simulation was conducted at each target temperature (300 K, 350 K, 400 K, and 450 K) for 7.5 ns followed by the NPT dynamics simulations at 1 atm for 7.5 ns each.

2.3. Thermomechanical properties

The mechanical properties of crosslinked epoxy, such as the elastic modulus and density, have shown crosslink-dependent trends in both experimental and computational works [13,14,50]; in other words, stiffness and density increase with the formation of crosslinks. In this study, the ratio between the number of reacted pairs and total possible pairs is defined as the crosslink density of MD model. Thus, a crosslink density of 66% was chosen for the bulk epoxy model with reasonable mechanical properties (elastic modulus and density) in comparison to experimental observations [52]. To derive the elastic moduli of the constructed epoxy systems, the Parrinello-Rahman fluctuation strain method was used [53].

The elastic modulus is obtained at a temperature of 300 K and pressure of 1 atm. The $N\sigma T$ ensemble simulation which uses Parrinello-Rahman barostat [53] is performed for 500 ps to fully relax the polymer network followed by a 100 ps $N\sigma T$ ensemble simulation under the same conditions. The obtained results are averaged over four different simulations for reliability. The detailed properties of chosen atomistic model is shown in Table 1.

The main idea of this study is to accelerate the transition event by elevating the temperature conditions in deriving the desired quasi-static yield stresses. However, it should be noted that the change in material properties caused by the phase transition should not occur within the elevated temperature range. Thus, in this study, the glass transition temperature (T_g) of the epoxy system is estimated from the density-temperature relationship by employing the same cooling-down method used in our previous study [21,25]. In particular, after the structural relaxation at 300 K and 1 atm, the unit cell is equilibrated at 600 K to reach the rubbery state under NVT and NPT ensemble simulations for 2 ns and 4 ns, respectively. Then, with a constant cooling down rate of 0.04 K/ps, the temperature of the unit cell is decreased to 100 K while monitoring the change of specific volume with respect to the variation of temperature. The glass transition temperature is predicted from the intersection point of the two linearly fitted lines of the specific volume-temperature profile, as shown in Fig. 4. By extending the two linear fitted lines for the glassy and rubbery states, the glass transition region can be determined from the intersection point located in the

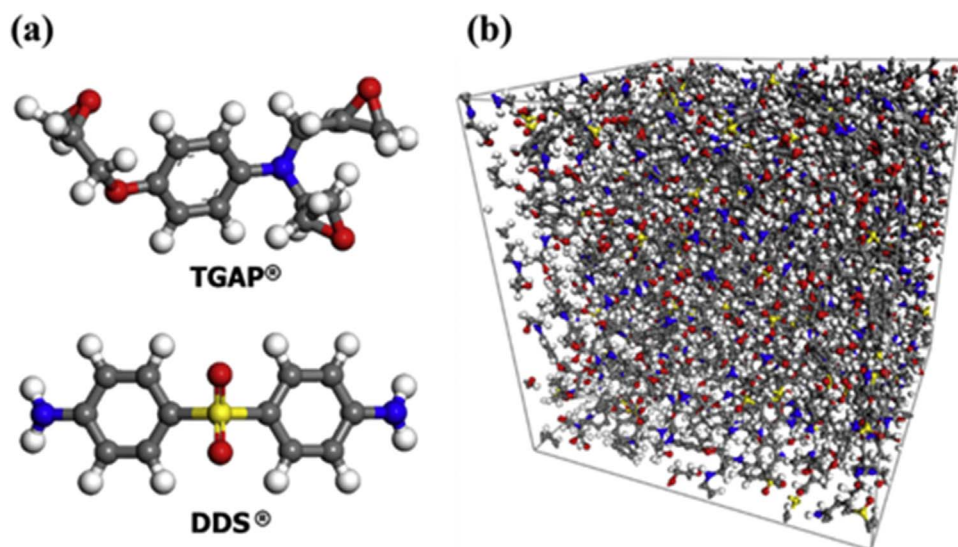


Fig. 2. Molecular structures of the (a) epoxy resin and curing agent. (b) A constructed atomistic model.

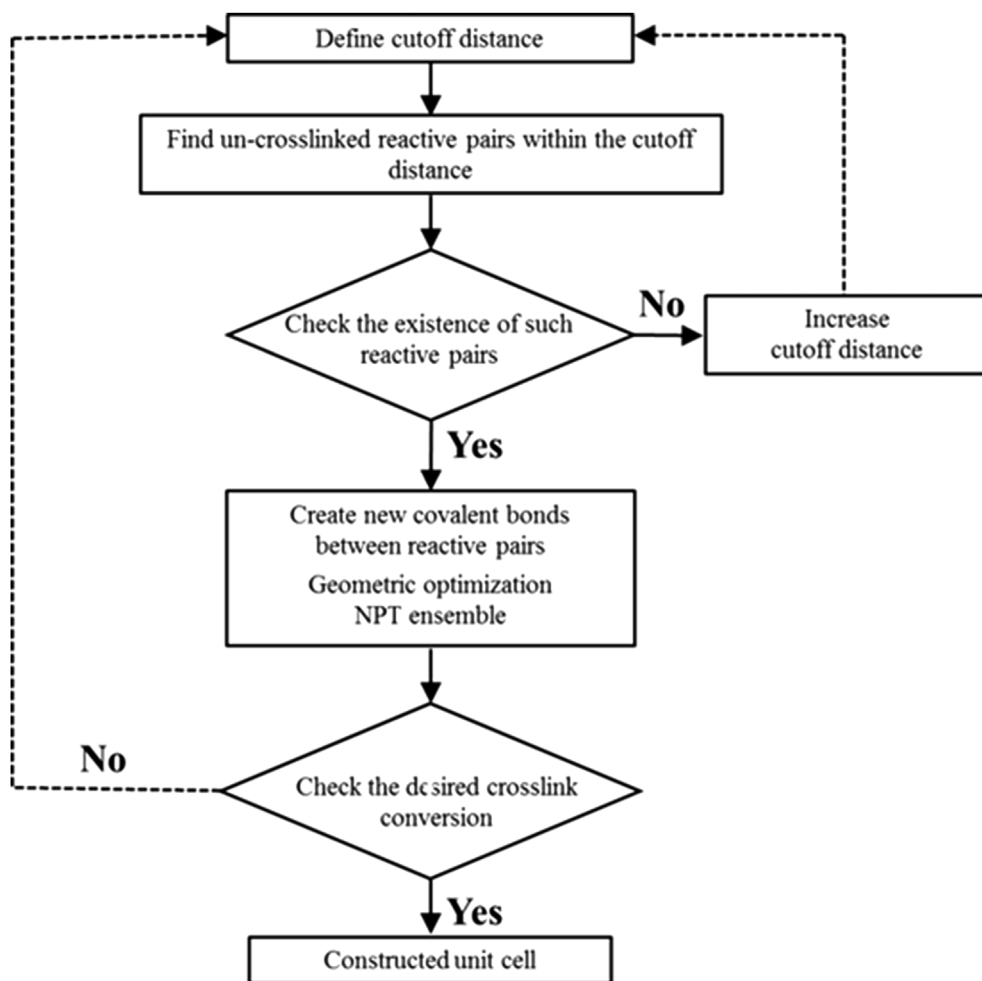


Fig. 3. A flowchart describing the simulation procedure of the dynamic crosslinking method.

temperature range between 480 K and 500 K, which is in a good agreement with the experimental results [54]. Considering the transition region, the available temperature for the glassy state is set to 450 K in this study.

2.4. Tensile simulation under different temperatures and strain rates

To derive the mechanical responses of the amorphous epoxy polymer, uniaxial tensile simulations under different strain rates and temperatures were performed. The basic scheme of the uniaxial tensile simulation is presented in Fig. 5. Under the external pressure on the planes normal to the tensile direction, strain is imposed gradually on

Table 1
Comparison of mechanical properties of TGAP/DDS epoxy system with those given in experimental literature.

| Present study | | | | Experiment (Gonzalez-Dominguez et al., 2011) | |
|--------------------------|---------|-------|-----------------------------|--|-----------------------------|
| 66% crosslinked TGAP/DDS | | | | | |
| E (GPa) | G (GPa) | ν | ρ (g/cm ³) | E (GPa) | ρ (g/cm ³) |
| 3.16 | 1.14 | 0.38 | 1.20 | 3.1–4.3 | 1.265 |

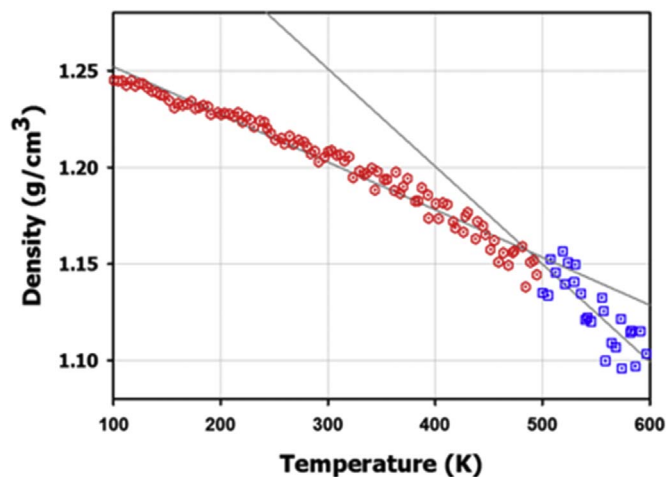


Fig. 4. Density-temperature relationship for the target epoxy system, which is used to obtain the glass transition temperature (intersection point).

the unit cell structure. Then, polymer chains in the unit cell deform along the tensile direction under certain strain rate conditions. To equilibrate the internal structure during the deformation, an *NPT* ensemble simulation is performed at every strain increment to describe Poisson's ratio by allowing the polymer chains to naturally shrink along the transverse direction. In this study, a strain of up to 0.15 is imposed in order to observe the elasto-plastic response sufficiently over different

temperatures and strain rates. The temperature was chosen below the glass transition temperature, from 300 K to 450 K with 50 K of interval; furthermore, various strain rates were examined for each temperature range. To obtain the distinct stress-strain responses, the simulation results were averaged from 6 to 36 times of independent production runs along all directions under an isotropic assumption.

3. Results and discussion

3.1. Stress-strain responses for glassy state under different strain rates and temperatures

Stress-strain profiles under different strain rates (10¹⁰/s, 10⁹/s, and 10⁸/s) and temperatures (300 K, 350 K, 400 K, and 450 K) were derived from MD simulations, as shown in Fig. 6(a–c). All the stress-strain curves show a similar material response in which stress increases linearly in the elastic range with increasing strain, and the increasing rate of stress is noticeably decreased. The studied material exhibits the elasto-plastic behavior without distinct strain softening, which differs from that of non-crosslinked thermoplastic polymers. In general, in the stress-strain response of the thermoplastic sample, distinct softening and hardening regions have been observed in other MD studies [33]. This difference can be attributed to the constrained chain mobility of the thermoset polymer generated by the crosslinked network, which hinders the softening of the polymer chain after the yield point.

As expected, the temperature and strain rate dependencies on the overall stress-strain profiles are well showcased in all profiles. As shown in Fig. 6(a–c), the overall stress decreases with increasing temperature and decreasing strain rate, which agrees with previous studies [4,34–44]. This result implies an important physical insight in MD simulations; namely, that both temperature and strain rate have an equivalent effect on the mechanical response of an amorphous polymer (from the viscoelastic point of view). In other words, the MD results certify that as a result of the equivalence of these two physical variables, the time scale (which is difficult to increase up to the quasi-static level in simulations) can be adjusted by changing the temperature; this agrees well with the experimental literature. For more detailed description of equivalence of the time and temperature, structural analyses were carried out by observing free volume and radius of gyration.

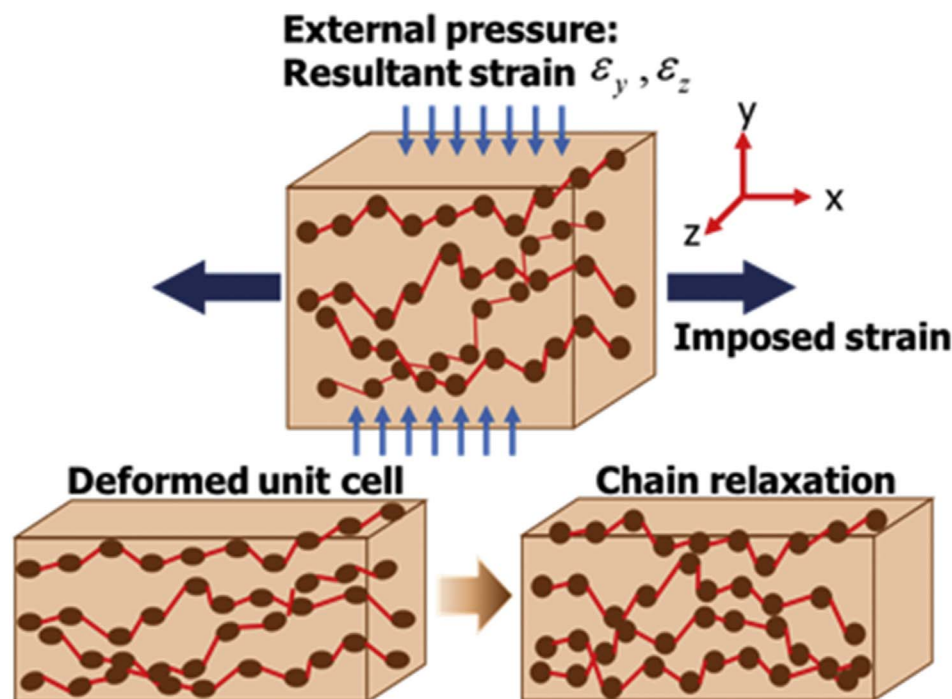


Fig. 5. A schematic of the uniaxial tensile simulation. Internal polymer chains are iteratively strained and relaxed using a multistep procedure.

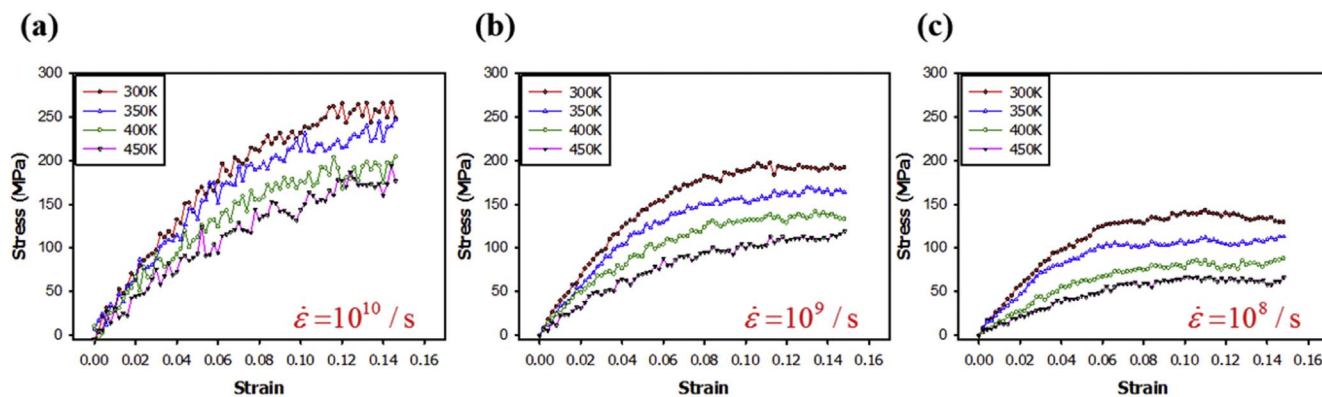


Fig. 6. Stress-strain responses obtained at various temperatures (below the glass transition temperature) and strain rates. The temperature/strain rate relationship is observed.

The results were provided in supporting information.

The exchange of these two physical variables can be understood from the perspective of the molecular movement of polymer chains. The elevated kinetic energy (which results from the increase of temperature) induces more vigorous molecular movement, which leads to the rapid structural rearrangement of polymer segments during the deformation. Similarly, as the strain rate decreases, polymer chains have more sufficient relaxation time to transform their internal structure from one state to another equilibrium state in the potential energy surface, leading to the same rearrangement. This crucially implies a pathway to overcome the limitation of MD simulations regarding their relatively short time scale (compared to the experimental counterpart). In other words, MD simulations with an elevated temperature generate a higher thermal activation energy that can compensate for the insufficient relaxation time of polymer chains caused by the inherently high strain rates.

3.2. Yield criterion

The distinct criterion for determining the yield point must be established to obtain the clear tendency of yield stress change from MD simulations. The yield of an amorphous polymer occurs when the polymer chain segments start to plastically flow to overcome the energy barrier for the local chains. Once the yield point is reached, various internal parameters such as dihedral angle, free volume, and angle are changed irreversibly as reported by previous studies [33,55]. Moreover, the deformation behavior of post-yield range of epoxy polymer can be dominated by the microcracking due to brittleness of epoxy networks. Due to the complex contribution of internal parameters, amorphous thermoset polymers are generally characterized by an unclear yield point (in contrast to crystalline materials) [42].

Thus, in order to determine the yield stress from the stress-strain curves of glassy polymers, we fitted the stress-strain data with a polynomial curve using a least-squares fit. Raw stress-strain data obtained from MD simulations (solid squares) are presented in Fig. 7 along with the fitted polynomial curve (purple solid line). Then, the fitted polynomial curve was fitted again by employing the linear elasto-plastic model where the stress behavior is described as two bilinear lines (elastic and linear plastic region). From the fitted linear elasto-plastic model, the Young's modulus, yield stress, and hardening parameters were determined as shown in Fig. 7. In the evaluation stage, we defined the residue of the stress as follows:

$$r(\sigma_Y, \varepsilon_Y, K) = \sigma - f^{E-P}(\sigma_Y, \varepsilon_Y, K), \text{ Minimize}|r|, \quad (3)$$

where f^{E-P} and σ are the linear elasto-plastic function and the stress of the epoxy in the polynomial fitted curve, respectively, and K is the hardening parameter. The yield stresses for each temperature and strain rate are provided in Table 2.

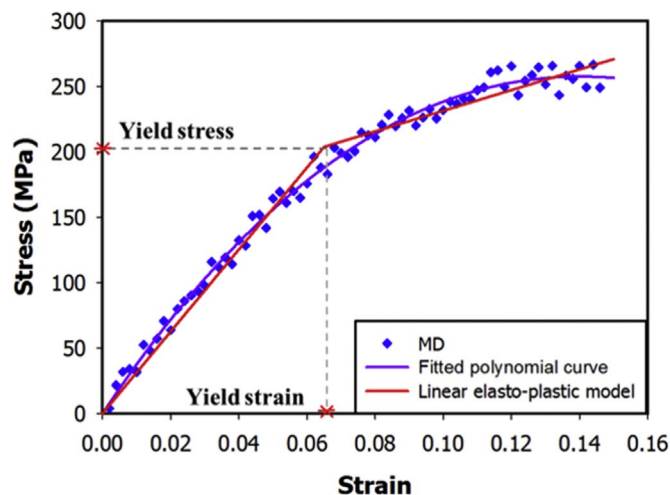


Fig. 7. A criterion for the yield point obtained from the stress-strain response. The yield point is determined by fitting the scattered MD data. The linear elasto-plastic model is composed of four degrees of freedom: Young's modulus, yield stress, yield strain and hardening exponent.

3.3. Prediction of quasi-static yield and its characteristics

3.3.1. Nonlinear characteristics of yield and their utilization with the MD result

Similar to the stress-strain responses, the derived yield stress values given in Fig. 8(a) demonstrate the temperature and strain rate-dependent characteristics; the yield stress linearly decreases with decreasing logarithmic strain rate and increasing temperature for the conditions considered in this work. This linearly decaying trend of yield stress in the computational environment corresponding to the variation of temperature was previously observed by Vu-Bac et al. [56] using MD simulations. More specifically, they obtained the yield stress of epoxy for the theoretical value of strain rate of $5 \times 10^9/s$ via MD simulations by employing the Argon theory, which was based on the assumption that the linearly decreasing trend of the yield stress with respect to temperature at high strain rates can be equally observed at the quasi-static conditions.

However, it should be noted that such linearity in the temperature-yield strength relationship cannot be guaranteed experimentally at extremely low temperatures where the molecular movements are severely frozen. This fact leads to the nonlinear variation of the yield stress with respect to the broad range of temperatures and strain rates. Bauwens-Crowet et al. [41] focused on this phenomenon and developed an experimental model for the yield of amorphous polymers by extending Eyring's model. In order to illustrate the yielding behavior at extremely low temperatures (from -150°C to 50°C in work of

Table 2
Yield data under different temperature and strain rate conditions for deriving quasi-static yield stress. For the accurate prediction of quasi-static yield, more detailed strain rate conditions of 300 K and 450 K are examined.

| Temperature (K) | Strain rate (/sec) | σ_y (MPa) | ϵ_y | σ_y/T (MPa/K) | Slope |
|-----------------|--------------------|------------------|--------------|----------------------|--------|
| 300 | 10^{11} | 289.63 | 0.138 | 0.9654 | 0.1112 |
| | $10^{10.5}$ | 238.10 | 0.077 | 0.7937 | |
| | 10^{10} | 203.82 | 0.065 | 0.6794 | |
| | $10^{9.5}$ | 185.36 | 0.066 | 0.6179 | |
| | 10^9 | 163.78 | 0.054 | 0.5459 | |
| | $10^{8.5}$ | 141.16 | 0.063 | 0.4705 | |
| 350 | 10^{10} | 174.89 | 0.059 | 0.4997 | 0.1112 |
| | 10^9 | 135.82 | 0.050 | 0.3881 | |
| | 10^8 | 97.05 | 0.043 | 0.2730 | |
| 400 | 10^{10} | 146.55 | 0.061 | 0.3664 | 0.0946 |
| | 10^9 | 109.20 | 0.057 | 0.2730 | |
| | 10^8 | 70.85 | 0.050 | 0.1771 | |
| 450 | $10^{11.5}$ | 275.09 | 0.114 | 0.6113 | 0.0643 |
| | 10^{11} | 204.12 | 0.130 | 0.4536 | |
| | 10^{10} | 117.47 | 0.061 | 0.2610 | |
| | 10^9 | 80.06 | 0.053 | 0.1779 | |
| | $10^{8.5}$ | 73.51 | 0.073 | 0.1634 | 0.0146 |
| | 10^8 | 58.61 | 0.066 | 0.1302 | |
| | $10^{7.5}$ | 37.07 | 0.034 | 0.0823 | |
| | 10^7 | 34.78 | 0.035 | 0.0773 | |
| | $10^{6.5}$ | 30.49 | 0.041 | 0.0678 | |

Bauwens-Crowet et al. [41]), it was assumed that the yield at this condition involves two independent rate processes, which have already been introduced in Eq. (2). In line with this approach, a cooperative model modified from Eyring's equation was also used to describe the yield stress-temperature relation of glassy polymers at a wide range of temperatures by Fortherigham and Cherry [46]. In their results, the same tendency was observed in which the yield stress nonlinearly varies over the broad range of strain rates and temperatures. This provides an important physical insight: namely, that the yield stress should vary nonlinearly over the broad range of strain rates; likewise, the yield stress varies nonlinearly with the variation of temperature. Therefore, nonlinearly varying yield stress according to the change of strain rate and temperature is obvious in the deformation kinetics of amorphous polymers, and also provides the logical basis for the TAD using a changeable shifting factor, which is proposed in this study for the first time.

To take into account the nonlinear characteristics of yield stress according to the temperature and strain rate on the environment of MD simulations, the profile for the reduced yield stress $\frac{\sigma_y}{T}$ versus $\log \dot{\epsilon}$ is

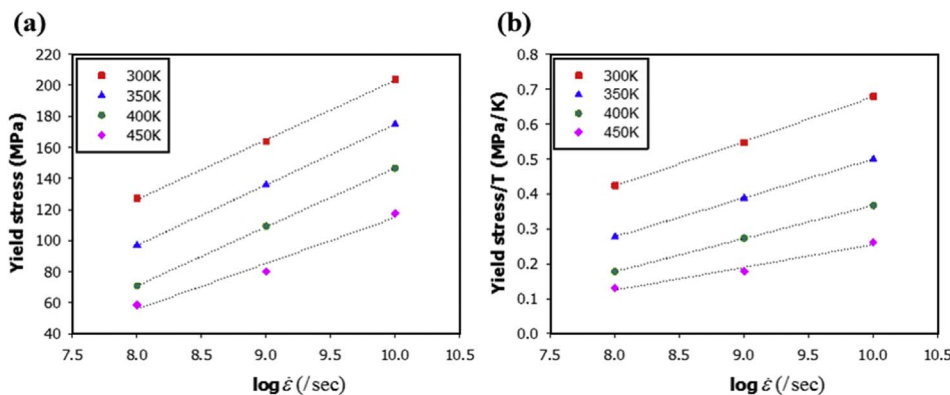


Fig. 8. Predicted (a) yield stress and (b) reduced yield stress at various strain rates and temperatures. The slopes of three points set in (b) are determined as 0.128 (300 K), 0.111 (350 K), 0.095 (400 K), and 0.064 (450 K).

plotted in Fig. 8(b) from the same data of Fig. 8(a). The slope of the reduced yield stress is also derived over the considered temperature conditions of this study in Table 2. The slope decreases with the increasing temperature from 0.128 at 300 K to 0.064 at 450 K. This decreasing slope of Fig. 8(b) is natural considering the abovementioned linear trend depicted in Fig. 8(a), since each slope is determined by the inverse of the given temperature.

Considering the abovementioned nonlinear varying trend of yield stress with strain rate, which is represented in the Eyring plot (Fig. 1), the slope of the reduced yield stress will steadily decrease as the strain rate decreases to the quasi-static level. Under the quasi-static rate conditions, the change of slope with respect to temperature is smaller than that of the high-rate conditions [40,41], since the sufficient structural relaxation time for inducing the viscous flow of polymer segments is guaranteed to initiate the yield, thereby resulting in low stress. Thus, the slope of reduced yield under quasi-static conditions must be lower than that under computational rate conditions. Furthermore, this trend can be confirmed by comparing the experimental results [40,41] with Fig. 8(b).

The obtained data imply that the slope of the reduced yield measured at the quasi-static conditions can be reached at high simulated strain rates, if the temperature is sufficiently elevated using the variation trend of the reduced yield with respect to temperature. In other words, the slope of the reduced yield (which is decreased by elevating temperature in MD simulations) is comparable with that obtained under the quasi-static conditions. In this study, owing to the equivalence between temperature and strain rate, changeable shift factors are obtained from the MD simulations by taking into account the nonlinear characteristics of yield stress. Subsequently, quasi-static yield can be estimated from the calculated shift factors.

3.3.2. Convergence of yield stress in lower strain rate range

To robustly predict quasi-static yield stress by constructing Eyring plot, the convergence of the reduced yield stress – strain rate plot should be guaranteed when the yield points at the high temperature range shift toward the lower strain rate. Accordingly, the slope of yield points at 300 K and higher strain rate range (higher than $10^8/s$) should be sufficiently decreased to the level at the experimentally lower strain rate range that is possibly determined from the yield points of 450 K. To confirm the convergence at 450 K, therefore, yield stresses were further examined with the various ranges of strain rates as given in Fig. 9. As mentioned in the previous section, the nonlinear relation between the yield stress and logarithmic strain rate is observed. Moreover, as far as the slope of yield stress with logarithmic strain rate is concerned, the data points can be separated into three groups (blue, green, and red points in Fig. 9). Unlike with lower temperature conditions, in a higher temperature range, the yield stresses of 450 K clearly show a relatively faster convergence with decreasing strain rate due to the contribution of temperature on the relaxation of polymer chains.

Thus, if the blue points in Fig. 9 (with a strain rate of computational

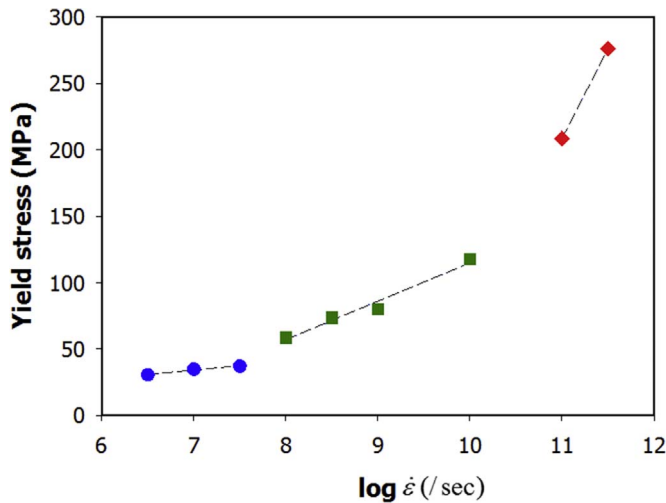


Fig. 9. Variation of yield stress depending on the strain rate under 450 K. The yield stresses can be divided into three groups according to the slope change.

scale at a higher temperature) are properly shifted toward the lower strain rate region that corresponds to an experimental strain rate range at the room temperature, the quasi-static yield stress can be reasonably obtained.

3.3.3. Shifting method and quasi-static (low strain rate) solution

In this section, a specific methodology for predicting quasi-static yield stress from high strain rate conditions is proposed for the first time by carefully considering the viscoelastic nature of amorphous polymers. The limitation of MD simulations regarding the time scale can be overcome by elevating the temperature based on the similarity of the slope of reduced yield between the quasi-static conditions and high-rate, elevated-temperature conditions. To take into account the nonlinear varying of yield stress with temperature and strain rate, the shifting method based on the ratio of changeable shifting factors are

introduced in this study. This method is based on the sequential shifting processes using the data sets in the elevated temperature conditions with the iterative algorithm to achieve the appropriate shifted positions of the given data sets.

The proposed method considers the involvement of multiple rate processes in the yield behavior of amorphous polymers, which means that the slope of the profile for the reduced yield stress versus logarithmic strain rate is constantly decreased with the decreasing strain rate in the MD simulations. Other researcher also observed the multiple rate processes regarding the polymer relaxation using the MD simulations [43]; Capaldi F. M. et al. carried out compressive tests using united atom model and observed nonlinear yield behavior with different temperatures. They indicated that the nonlinear feature observed in MD simulations is a clear evidence of multiple rate processes in polymer yield behavior. Based on the assumption that the yield behavior of amorphous polymers under the wide range of strain rate is significantly involved with the multiple rate processes, the changeable shifting factor concept are introduced in the present study. Herein, to take into account the multiple rate processes in polymer yielding behavior, the correlation among yield stress, strain rate, and temperature is described as an exponentially decaying function:

$$\frac{\sigma_y}{T} = a \cdot \exp(b \cdot \log \dot{\epsilon}) + c \cdot \log \dot{\epsilon} + d, \tag{4}$$

where, a , b , c , and d are fitting coefficients. Compared to the Ree-Eyring model in Eq. (1), the present model is composed of exponential terms instead of using arc hyperbolic sine function to consider the nonlinear nature of multiple rate processes. The linear term in Eq. (4) is to illustrate the extinction of nonlinearity in yield stress for the extremely low strain rate condition, which is similar to the Ree-Eyring model.

Detailed description to predict quasi-static yield using the iterative regime is shown in Fig. 10. The present acceleration method is based on the sequential shifting concept; the data points at a higher temperature can be shifted sequentially to a lower strain rate range using the shifting factor ratio calculated from the existing fitted curve (shifting factors are derived by Eq. (2)). In the shifting procedure, the selection of data points require a profound consideration; the proper data points showing

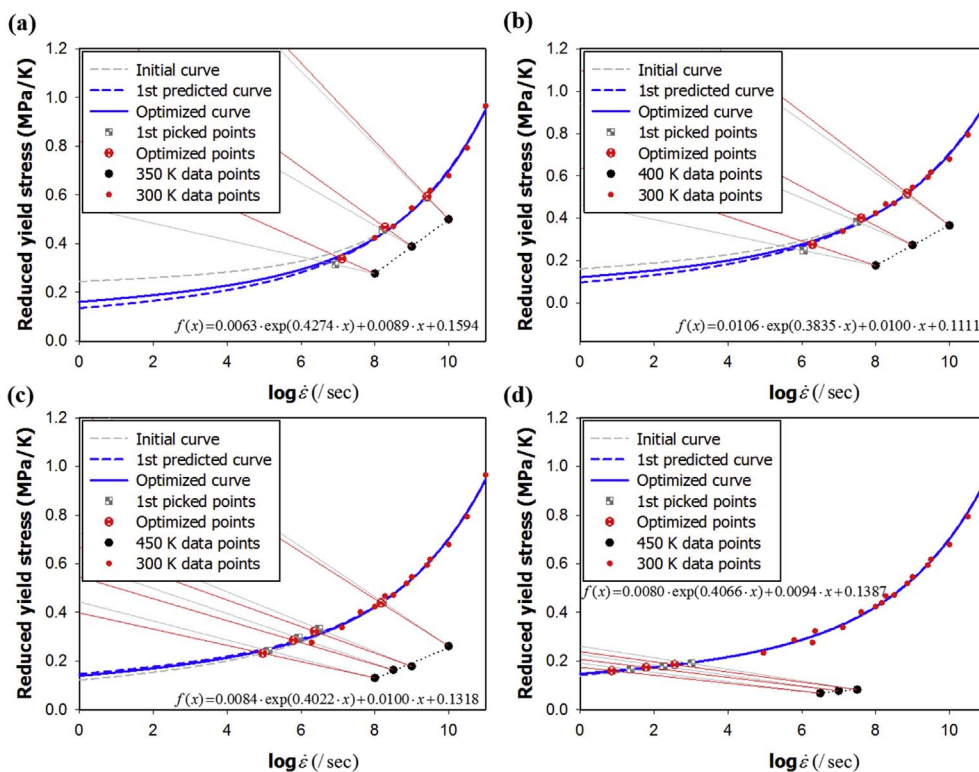


Fig. 10. Illustration of construction process of Eyring plot for the reference temperature (300 K). Reduced yield stresses under elevated temperatures ((a) 350 K, (b) 400 K, and (c), (d) 450 K) are shifted to a lower strain rate range based on the derived shifting factor ratio. At each shifting step, the prediction profile is updated iteratively to achieve the appropriate modification of prediction curve. The fitted equation for the final updated curve for each step are given in the figures.

the linearly decaying trend need to be determined which represent the same rate processes.

Herein, once the data points set is shifted to the existing fitting curve, the constant slope trend should be maintained to represent the same rate processes. The data points in the shifted condition were derived by minimizing the deviation between the shifted point at the highest strain rate and existing fitting curve using the least square method.

However, the accuracy would not be guaranteed in the first shifted points since the existing fitting curve may not be able to properly predict the yield stress of the lower strain rate range. Thus, the shifting of data sets should be performed iteratively with an appropriate modification of the prediction curve. In the present study, the existing fitting curve was iteratively updated using the shifted data sets to describe the nature of rate process of considered temperature condition. Among the revised candidates of fitting curve, the most appropriate curve was determined to show a minimum deviation between the shifted points and candidate curve. This iterative modification of fitting curve was conducted for at least 30 times at each elevated temperature condition. Finally, the quasi-static yield stress was properly predicted through the sequential shifting of yield in higher temperature conditions based on the iterative modification of prediction curve.

When it comes to applying the present method, the following features need to be considered for the robust and accurate estimation. First, when selecting the data set, the linearity should be guaranteed to demonstrate the same nature of rate process. Plus, the prediction region should be magnified sequentially from the initial region where the deviation of nature in the rate process is minimal. Moreover, the more proper estimation of yield stress will be possible with the more yield stress points, especially for the region showing larger deviation in the nature of rate process. In this regard, the validation of proposed method is conducted at the end of section by the comparison between the full and limited data sets.

Yield points at 300 K were derived from $10^8/s$ to $10^{11}/s$ at the interval of $10^{0.5}/s$ and fitted with Eq. (4) as shown with grey dash line in Fig. 10(a). Based on the previous shifting factor method of two rate processes [40,41], each shifting factor ratio for the data points of 350 K is derived and represented by the grey solid lines in Fig. 10(a). Taking these solid lines as a guideline, the data set was shifted while maintaining its original slope. As can be seen in Fig. 10(a), the first shifted points (grey square points) are deviated from the initial prediction curve (grey dash line). It means that in fact, the initial prediction curve is not enough to predict the yield of lower strain rate range. Thus, the initial prediction curve is modified with the shifted points as shown with blue dash line in Fig. 10(a). Following the iterative update process with the data set of 350 K, the most appropriate curve is determined with the final shifted points (red circle points) and shown with blue solid line in Fig. 10(a). Comparing with the previous prediction curve shown with grey dash line in Fig. 10(a), the updated curve displays quite different quasi-static yield stress in a lower strain rate range. With the same manner, the data points in 400 K and 450 K were shifted and the fitting curve was iteratively updated.

One thing to be noted is that the data points for 450 K was divided into two groups depending on their slope as discussed in section 3.3.2. Since the change in yield stresses with the strain rate is nonlinear in this case, we separated the obtained raw data into two groups having different slope respectively and then applied the shifting process for each group.

From the present shifting method, the profile for the shifted yield stress along the logarithmic strain rate is constructed at the target temperature (300 K) in Fig. 11(a). With the shifted strain rate condition, the ultimate tensile strength is also plotted in Fig. 11(b). Interestingly, the ultimate tensile stress decreases more rapidly than the yield stress. This behavior is likely to be attributed to the more relaxed state of the post-yield region. Lastly, as shown in Fig. 11, the two predicted values show a good agreement with the experimental results, which are

represented by the dotted line. From the present model, we expect that the effect of physical parameters influencing the yielding of amorphous polymers as reported in the previous literature can be further considered, such as crosslinking ratio [13,57], crosslinking method [13], and system size [57].

To confirm the robustness of proposed method, we compared the predicted results from the full data sets (identical data sets with Fig. 11(a)) and limited data sets. The following data sets for yield stresses are considered for the case of using limited data sets: $10^{10}/s$, $10^8/s$ (350 K), $10^{10}/s$, $10^8/s$ (400 K), and $10^{10}/s$, $10^9/s$, $10^8/s$, $10^{7.5}/s$, $10^{6.5}/s$ (450 K). In total, four points are omitted for the limited data set to compare with the result of using the full data sets. Although the data points are omitted, the slope of each data set at reduced yield versus logarithmic strain rate profile is maintained without showing a significant deviation. The predicted yield stresses with the strain rate for the cases of full data sets and limited data sets are given in Fig. 12, showing almost identical trend. Only minor difference (about 2 MPa) is observed under the quasi-static strain rate range. The application of many intermediate data points to the shifting procedure can possibly improve the accuracy of yield stress evolution. As far as the overall trend in yield stresses is concerned, the omission of intermediate points in the data set does not hinder the prediction of quasi-static yield and overall yield evolution with varying strain rate when the linearity is ensured in the limited data set. Above all, the most important point in predicting of quasi-static yield is that the overall accuracy can be substantially enhanced by deriving more yield stress points which can be shifted to the quasi-static strain rate region.

3.3.4. Quasi-static (low rate) stress-strain equation via established yield model

The quasi-static mechanical response can be estimated via the suggested yield model by considering the quasi-static elastic and hardening law. Since the elastic modulus generally varies with the strain rate, as reported in previous studies [36,58], the quasi-static elastic modulus must be determined in an MD environment in order to establish the stress-strain profile. Therefore, the modulus under the reference state (300 K) without any rate effect was obtained from the Parrinello-Rahman fluctuation strain method, which was introduced in Section 2.3.

To describe the plastic response of the epoxy polymer, Ludwick's hardening model is adopted according to the following form:

$$\sigma_e = \sigma_Y + h(\varepsilon^P)^n, \quad (5)$$

where σ_e , h , ε^P , and n are the von Mises's effective stress, strength coefficient, effective plastic strain, and hardening exponent, respectively. As well as the elastic modulus, the hardening of glassy polymers under $10^{10}/s$, $10^9/s$, and $10^8/s$ conditions (at 300 K) also indicates the rate-dependent characteristics, as reported by previous studies [59–61]. The values of h and n rapidly decrease as the strain rate decreases to $10^8/s$, indicating that the slope of the plastic strain range in the stress-strain response significantly decreases. When considering the monotonically hardened plastic behavior of thermoset polymers, this trend also can be explained in terms of the yield model by noting that the distinction between the ultimate tensile strength and yielding quickly becomes constant as the rate decreases as shown in Fig. 11(b). In this manner, quasi-static h and n values were determined via exponential fitting by reflecting the rapid convergence.

Finally, the uniaxial tensile behavior of the epoxy polymer was derived, as shown in Fig. 13. The quasi-static yield stress, yield strain, Young's modulus, and hardening parameters (h , n) were determined to be 48.12 MPa, 1.52%, 3.17 GPa, 40.81, and 0.44, respectively. The proposed model shows good agreement with the experimental stress-strain profiles [51,52]. The quasi-static yield strain is found to be about 1.52%, which represents a drop by about 4–5% (as compared to the computational rate conditions) and is attributed to the strain rate dependency on the yield strain as reported in previous study [62]. In

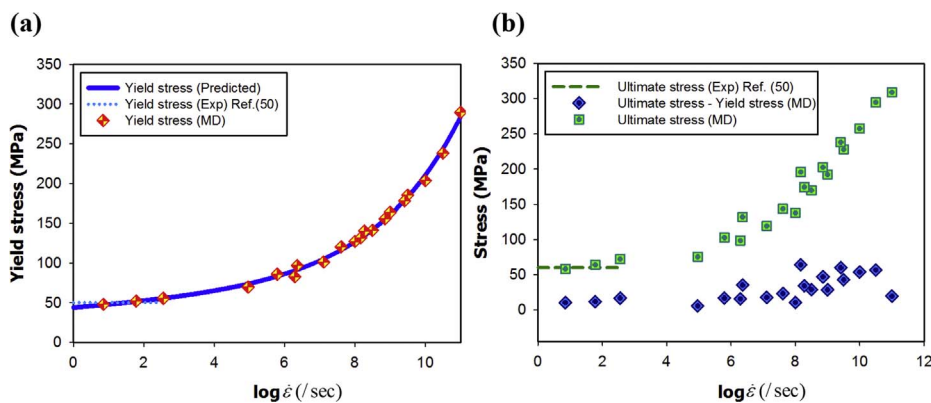


Fig. 11. Predicted yield stress (a) and corresponding ultimate stress (b) changes with variation of the strain rate. The obtained curves show good agreements with the magnitudes of the experimental yield stress (50.19 MPa) and ultimate response (60 MPa), which are obtained from the quasi-static response (experimental test) of epoxy by applying the suggested yield criterion.

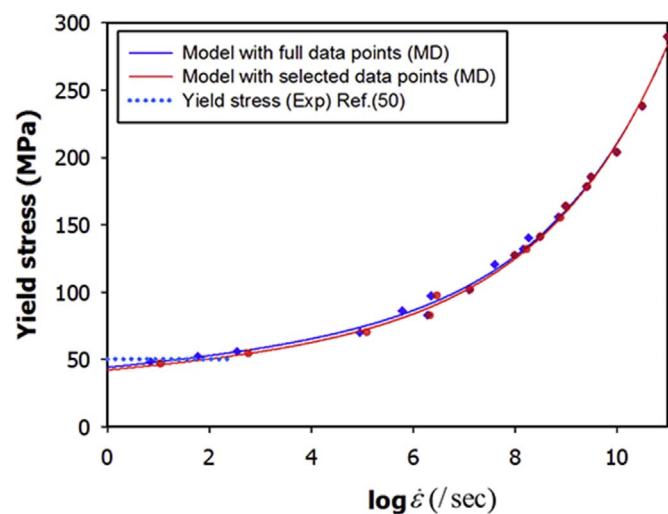


Fig. 12. Comparison of prediction profiles between models of using full data points (identical curve in Fig. 11(a)) and limited data points.

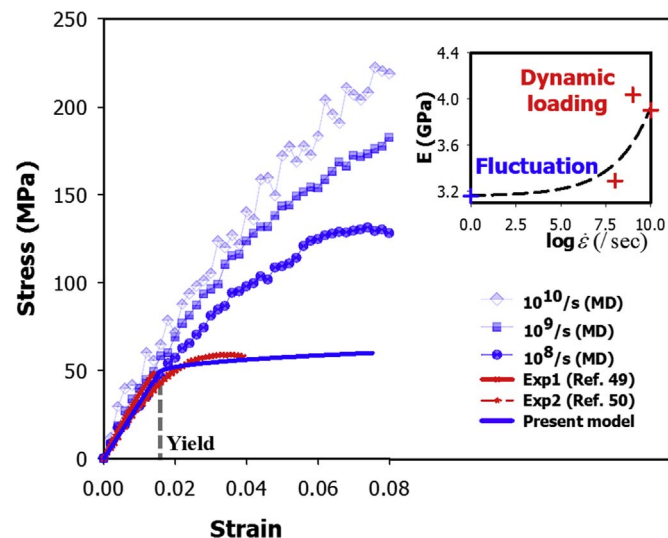


Fig. 13. A comparison of the predicted quasi-static (experimental low strain rate) stress-strain solution (blue solid line) with the experimental results. The inset depicts the exponentially fitted Young's modulus as a function of strain rate. (For interpretation of the references to colour in this figure legend, the reader is referred to the Web version of this article.)

addition, the suggested quasi-static model can describe the rate effect by considering the rate-dependent elastic and hardening law, which can be derived from the exponential form.

4. Conclusion

An accelerated method to predict the quasi-static (experimental low strain rate) rate yield from the full-atomic MD simulation has been established by employing the concept of Eyring theory for the yield of amorphous polymer systems. Using the stress-strain responses of amorphous epoxy polymers under different temperatures and strain rates, the yield stress of each strain rate and temperature can be obtained with the linear elasto-plastic yield criterion. In order to take the nonlinear characteristics of the yield stress into consideration, shifting factor ratios were calculated and applied to shift the yield at the elevated temperature toward the lower strain rate conditions at the target temperature based on the derived trend for the slope of the reduced yield.

The quasi-static yield stress (in accordance with the derived shifting factor ratios) was estimated through the MD simulations and validated with previous experiments, showing good nonlinear rate-dependent behavior. The suggested yield model opens an avenue for establishing a quasi-static stress-strain response with the rate-dependent elasto-plastic law in an MD environment.

The temperature-accelerated MD scheme will serve to break through an inherent strain rate-dependent discrepancy between computational work and experimental work, and in particular to describe the viscoelastic nature of polymer yielding. The present shifting method provides an accurate prediction regarding the quasi-static yield behavior and structural relaxation of amorphous polymers. Furthermore, the result of full-atomic MD simulations can be utilized to construct a multiscale bridging method for the efficiency of design by adopting continuum models that can describe the nanophenomena. In this manner, the suggested method makes MD simulations more powerful for polymer material design in that it can be used not only for qualitative analysis of the nanophenomena, but also for quantitative predictions of deformation mechanics. That is because the present method is not limited to epoxy systems, but can be used to estimate the quasi-static solution for yield efficiently for any type of amorphous polymer system.

Acknowledgments

This work was supported by the National Research Foundation of Korea (NRF) grant funded by the Korea government (MSIP) (No. 2012R1A3A2048841).

References

- [1] Johnsen BB, Kinloch AJ, Mohammed RD, Taylor AC, Sprenger S. Toughening mechanisms of nanoparticle-modified epoxy polymers. *Polymer* 2007;48(2):530–41.
- [2] Bandyopadhyay A, Valavala PK, Clancy TC, Wise KE, Odegard GM. Molecular modeling of crosslinked epoxy polymers: the effect of crosslink density on thermomechanical properties. *Polymer* 2011;52(11):2445–52.
- [3] Poulain X, Benzerga AA, Goldberg RK. Finite-strain elasto-viscoplastic behavior of

- an epoxy resin: experiments and modeling in the glassy regime. *Int J Plast* 2014;62:138–61.
- [4] Sundararaghavan V, Kumar A. Molecular dynamics simulations of compressive yielding in cross-linked epoxies in the context of Argon theory. *Int J Plast* 2013;47:111–25.
- [5] Shenogina N, Tsige M, Patnaik SS, Mukhopadhyay SM. Molecular modeling approach to prediction of thermo-mechanical behavior of thermoset polymer networks. *Macromolecules* 2012;45(12):5307–15.
- [6] Kim B, Choi J, Yang S, Yu S, Cho M. Multiscale modeling of interphase in cross-linked epoxy nanocomposites. *Composites Part B* 2017;120(1):128–42.
- [7] Ahmadi M, Masoomi M, Safi S. Mechanical property characterization of carbon nanofiber/epoxy nanocomposites reinforced by GMA-grafted UHMWPE fibers. *Composites Part B* 2015;83:43–9.
- [8] Moghadam RM, Saber-Samandari S, Hosseini SA. On the tensile behavior of clay-epoxy nanocomposite considering interphase debonding damage via mixed-mode cohesive zone material. *Composites Part B* 2016;89:303–15.
- [9] Wong M, Paramsothy M, Xu XJ, Ren Y, Li S, Liao K. Physical interactions at carbon nanotube-polymer interface. *Polymer* 2003;44:7757–64.
- [10] Gou J, Liang Z, Zhang C, Wang B. Computational analysis of effect of single-walled carbon nanotube rope on molecular interaction and load transfer of nanocomposites. *Composites Part B* 2005;36(6–7):524–33.
- [11] Varshney V, Patnaik SS, Roy AK, Farmer BL. A molecular dynamics study of epoxy-based networks: cross-linking procedure and prediction of molecular and material properties. *Macromolecules* 2008;41:6837–42.
- [12] Masoumi S, Arab B, Valipour H. A study of thermo-mechanical properties of the cross-linked epoxy: an atomistic simulation. *Polymer* 2015;70:351–60.
- [13] Kim B, Choi J, Yang S, Yu S, Cho M. Influence of crosslink density on the interfacial characteristics of epoxy nanocomposites. *Polymer* 2015;60:186–97.
- [14] Li C, Strachan A. Evolution of network topology of bifunctional epoxy thermosets during cure and its relationship to thermo-mechanical properties: a molecular dynamics study. *Polymer* 2015;75:151–60.
- [15] Ko MB, Jo WH. Effect of reactivity on cure and phase separation behavior in epoxy resin modified with thermoplastic polymer: a Monte Carlo simulation approach. *Macromolecules* 1994;27:7815–24.
- [16] Khanna U, Chanda M. Monte Carlo simulation of network formation based on structural fragments in epoxy-anhydride systems. *Polymer* 1996;37(13):2831–44.
- [17] Ahangari MG, Fereidoon A, Ganji MD. Density functional theory study of epoxy polymer chains adsorbing onto single-walled carbon nanotubes: electronic and mechanical properties. *J Mol Model* 2013;19:3127–34.
- [18] Li C-C, Lu C-L, Lin Y-T, Wei B-Y, Hsu W-K. Creation of interfacial phonons by carbon nanotube-polymer coupling. *Phys Chem Chem Phys* 2009;11:6034–7.
- [19] Shin H, Chang S, Yang S, Youn BD, Cho M. Statistical multiscale homogenization approach for analyzing polymer nanocomposites that include model inherent uncertainties of molecular dynamics simulations. *Composites Part B* 2016;87:120–31.
- [20] Yang S, Yu S, Ryu J, Cho J-M, Kyung W, Han D-S, Cho M. Nonlinear multiscale modeling approach to characterize elastoplastic behavior of CNT/polymer nanocomposites considering the interphase and interfacial imperfection. *Int J Plast* 2013;41:124–46.
- [21] Yu S, Yang S, Cho M. Multi-scale modeling of cross-linked epoxy nanocomposites. *Polymer* 2009;50:945–52.
- [22] Choi J, Shin H, Yang S, Cho M. The influence of nanoparticle size on the mechanical properties of polymer nanocomposites and the associated interphase region: a multiscale approach. *Compos Struct* 2015;119:365–76.
- [23] Yu S, Yang S, Cho M. Analysis of thermal conductivity of polymeric nanocomposites under mechanical loading. *J Appl Phys* 2013;114:213503.
- [24] Ionita M. Multiscale molecular modeling of SWCNTs/epoxy resin composites mechanical behavior. *Composites Part B* 2012;43(8):3491–6.
- [25] Choi J, Yu S, Yang S, Cho M. The glass transition and thermoelastic behavior of epoxy-based nanocomposites: a molecular dynamics study. *Polymer* 2011;52:5197–203.
- [26] Rahman R, Haque A. Molecular modeling of crosslinked graphene-epoxy nanocomposites for characterization of elastic constants and interfacial properties. *Composites Part B* 2013;54:353–64.
- [27] Eyring H. Viscosity, plasticity, and diffusion as examples of absolute reaction rates. *J Chem Phys* 1936;4:283–91.
- [28] Robertson RE. Theory for the plasticity of glassy polymers. *J Chem Phys* 1966;44:3950–6.
- [29] Bowden PB, Raha S. A molecular model for yield and flow in amorphous glassy polymers making use of dislocation analogue. *Phil Mag* 1974;29(1):149–66.
- [30] Argon AS. A theory for the low-temperature plastic deformation of glassy polymers. *Phil Mag* 1973;28(4):839–65.
- [31] Argon AS. Physical basis of distortional and dilatational plastic flow in glassy polymers. *J Macromol Sci Part B* 1973;8:563–96.
- [32] Mott P, Argon AS, Suter U. Atomistic modelling of plastic deformation of glassy polymers. *Phil Mag* 1993;67(4):931–78.
- [33] Hossain D, Tschopp MA, Ward DK, Bouvard JL, Wang P, Horstemeyer MF. Molecular dynamics simulations of deformation mechanisms of amorphous polyethylene. *Polymer* 2010;51(25):6071–83.
- [34] Gómez-del Río T, Rodríguez J. Compression yielding of epoxy: strain rate and temperature effect. *Mater Des* 2012;35:369–73.
- [35] Krempl E, Khan F. Rate(time)-dependent deformation behavior: an overview of some properties of metals and solid polymers. *Int J Plast* 2003;19:1069–95.
- [36] Richeton J, Ahzi S, Vecchio KS, Jiang FC, Makradi A. Modeling and validation of the large deformation inelastic response of amorphous polymers over a wide range of temperatures and strain rates. *Int J Solids Struct* 2007;44:7938–54.
- [37] Richeton J, Ahzi S, Daridon L, Rémond Y. A formulation of the cooperative model for the yield stress of amorphous polymers for a wide range of strain rates and temperatures. *Polymer* 2005;46:6035–43.
- [38] Richeton J, Ahzi S, Vecchio KS, Adharapurapu RR. Influence of temperature and strain rate on the mechanical behavior of three amorphous polymers: characterization and modelling of the compressive yield stress. *Int J Solids Struct* 2006;43:2318–35.
- [39] Richeton J, Ahzi S, Vecchio KS, Jiang FC, Makradi A. Modeling and validation of the large deformation inelastic response of amorphous polymers over a wide range of temperatures and strain rates. *Int J Solids Struct* 2007;44:7938–54.
- [40] Bauwens-Crowet C, Bauwens JC, Homès G. Tensile yield-stress behavior of glassy polymers. *J Polym Sci A2* 1969;7:735–42.
- [41] Bauwens-Crowet C, Bauwens JC, Homès G. The temperature dependence of yield of polycarbonate in uniaxial compression and tensile tests. *J Mater Sci* 1972;7:176–83.
- [42] Odegard GM, Jensen BD, Gowtham S, Wu J, He J, Zhang Z. Predicting mechanical response of crosslinked epoxy using ReaxFF. *Chem Phys Lett* 2014;591:175–8.
- [43] Capaldi FM, Boyce MC, Rutledge GC. Molecular response of a glassy polymer to active deformation. *Polymer* 2004;45:1391–9.
- [44] Yagyu H. Coarse-grained molecular dynamics simulation of the effects of strain rate on tensile stress of crosslinked rubber. *Soft Mater* 2015;13(4):263–70.
- [45] Ree T, Eyring H, Eirich FR, editor. *Rheology*, vol. 2. New York: Academic Press; 1958 [chapter 3].
- [46] Fotheringham D, Cherry BW. The role of recovery forces in the deformation of linear polyethylene. *J Mater Sci* 1978;13:951–64.
- [47] Heine DR, Grest GS, Lorenz CD, Tsige M, Stevens MJ. Atomistic simulations of end-linked poly(dimethylsiloxane) networks: structure and relaxation. *Macromolecules* 2004;37(10):3857–64.
- [48] Demir B, Walsh TR. A robust and reproducible procedure for cross-linking thermoset polymers using molecular simulation. *Soft Matter* 2016;12(8):2453–64.
- [49] Tam L-h, Lau D. A molecular dynamics investigation on the cross-linking and physical properties of epoxy-based materials. *RSC Adv* 2014;4(62):33074–81.
- [50] Levita G, Petris SD, Marchetti A, Lazzeri A. Crosslink density and fracture toughness of epoxy resins. *J Mater Sci* 1991;26:2348–52.
- [51] Gonzalez-Dominguez JM, Anson-Casas A, Diez-Pascual AM, Ashrafi B, Naffakh M, Backman D, et al. Solvent-free preparation of high-toughness epoxy-SWNT composite materials. *ACS Appl Mater Interfaces* 2011;3:1441–50.
- [52] Gonzalez-Dominguez JM, Diez-Pascual AM, Anson-Casas A, Gomez-Fatou MA, Martinez MT. Epoxy composites with covalently anchored amino-functionalized SWNTs: towards the tailoring of physical properties through targeted functionalization. *J Mater Chem* 2011;21:14947–58.
- [53] Parrinello M, Rahman A. Crystal structure and pair potentials: a molecular dynamics study. *Phys Rev Lett* 1980;45(14):1196–9.
- [54] Pethrick RA, Hollins EA, McEwan I, MacKinnon AJ, Hayward D, Cannon LA. Dielectric, mechanical and structural, and water absorption properties of a thermoplastic-modified epoxy resin: poly(ether sulfone)-amine cured epoxy resin. *Macromolecules* 1996;29:5208–14.
- [55] Jatin, Sudarkodi V, Basu S. Investigations into the origins of plastic flow and strain hardening in amorphous glassy polymers. *Int J Plast* 2014;56:139–55.
- [56] Vu-Bac N, Bessa MA, Rabczuk T, Liu WK. A multiscale model for the quasi-static thermo-plastic behavior of highly cross-linked glassy polymers. *Macromolecules* 2015;48(18):6713–23.
- [57] Shenogina NB, Tsige M, Patnaik SS, Mukhopadhyay SM. Molecular modeling approach to prediction of thermo-mechanical behavior of thermoset polymer networks. *Macromolecules* 2012;45(12):5307–15.
- [58] Nazarychev VM, Lyulin AV, Larin SV, Gurtovenko AA, Kenny JM, Lyulin SV. Molecular dynamics simulations of uniaxial deformation of thermoplastic polyimides. *Soft Matter* 2016;12:3972.
- [59] G Sell C, Jonas JJ. Yield and transient effects during the plastic deformation of solid polymers. *J Mater Sci* 1981;16:1956–74.
- [60] Wendlandt M, Tervoort TA, Suter UW. Non-linear, rate-dependent strain-hardening behavior of polymer glasses. *Polymer* 2005;46(25):11786–97.
- [61] Hope PS, Ward IM, Gibson AG. The hydrostatic extrusion of poly-methylmethacrylate. *J Mater Sci* 1980;15:2207–20.
- [62] Stachurski ZH. Deformation mechanisms and yield strength in amorphous polymers. *Prog Polym Sci* 1997;22:407–74.